Journal of Hazardous Materials 174 (2010) 314–322

Contents lists available at ScienceDirect

Journal of Hazardous Materials

journal homepage: www.elsevier.com/locate/jhazmat

Electrochemical treatment of phenolic waters in presence of chloride with boron-doped diamond (BDD) anodes: Experimental study and mathematical model

Michele Mascia*, Annalisa Vacca, Anna Maria Polcaro, Simonetta Palmas, Jesus Rodriguez Ruiz, Anna Da Pozzo

Dipartimento di Ingegneria Chimica e Materiali, Università di Cagliari Piazza d'Armi 09123 Cagliari, Italy

ARTICLE INFO

Article history:
Received 2 July 2009
Received in revised form
10 September 2009
Accepted 11 September 2009
Available online 17 September 2009

Keywords:
Mathematical model
Electrochemical treatment
BDD
Chloride
m-Cresol

ABSTRACT

This work deals with an experimental and numerical study on the electrochemical treatment of waters containing phenolic compounds with boron-doped diamond (BDD) anodes.

Anodic oxidation of m-cresol, as a model of phenolic compound, was investigated by galvanostatic electrolyses. The electrolyses were carried out under different experimental conditions by using an impinging-jet flow cell inserted in a hydraulic circuit in a closed loop. On the basis of the experimental results a mathematical model was implemented to simulate the effect of the chemistry of organic compounds and solution on the process, in particular the effect of chlorides on the kinetics of m-cresol oxidation. The effect of hydrodynamics of the cell on the mass transfer towards the electrode surface was also considered.

The model was validated through comparison with experimental data: the results showed that the proposed model well interpreted the complex effect on removal efficiency of such operative parameters as current density, hydrodynamic of the reactor and chemistry of the solution.

The model predictions were utilised to obtain quantitative information on the reaction mechanism, as well as to predict the performance of the process under different operative conditions, by calculating some relevant figures of merit.

1. Introduction

The electrochemical treatment of water and wastewater with boron-doped diamond (BDD) anode has been extensively studied for the removal of toxic and biorefractory organic compounds [1–3] or for disinfection and purification of natural waters [4–6].

In the oxidative process at BDD several series/parallel steps may be involved [7–9]: direct electron exchange may occur at the electrode surface simultaneously with the decomposition of water to hydroxyl radicals. OH radicals are weakly sorbed at BDD surface [8,9] and may react with the organic compounds in a thin layer close to the anodic surface: this pseudo-surface reaction can oxidise organic compounds in one or more stages up to mineralization. Moreover, the OH radicals can lead to the formation of reactive oxygen species which can oxidise the organic matter in the bulk of the solution [5] or may give oxygen.

The role of chloride ions is of particular concern; they are usually present in waters and can be oxidised at the anode surface to form active chlorine species. The oxidation mediated by active chlorine electrogenerated species has been widely studied also using BDD anodes [10]. At low chloride concentration, the disinfection or purification processes are mediated by active chlorine ($HClO/ClO^-$ and ClO_2), but the formation of chlorite, chlorate and perchlorate ions as disinfection by-products is also possible. In the removal of organics from water some authors [11] reported a positive effect of chloride ions, indicating that the active chlorine produced at the anode can give a bulk contribution to the overall oxidation process. Other researches found a decrease in the process efficiency [12] in presence of Cl^-, which was attributed to the different reactivity of the compounds, and to the competition between chloride oxidation and OH radical generation [10].

In order to quantify the complex phenomena involved in the oxidative process different mathematical models of the electrochemical treatment with BDD anodes were proposed [7,13,14]. A diffusion-reaction model was developed in our previous work and it was used to interpret experimental data deriving from electrolyses of several organic compounds [15]. The effects of hydrodynamics of the cell, current density and chemistry of the

* Corresponding author. Tel.: +39 0706755052; fax: +39 0706755067.
E-mail address: michele.mascia@unica.it (M. Mascia).

0304-3894/$ – see front matter © 2009 Elsevier B.V. All rights reserved.
doi:10.1016/j.jhazmat.2009.09.053

Nomenclature

List of symbols

a	specific electrode area $a = (A/V_R)$ (m^{-1})
A	anode area (m^2)
C_i	concentration of the ith compound (mol m^{-3})
d	nozzle diameter (m)
v	linear velocity in the nozzle (m s^{-1})
ρ	density of electrolyte (kg m^3)
μ	viscosity of electrolyte (kg m^{-1} s^{-1})
D_i	diffusivity of the ith compound (m^2 s^{-1})
F	Faraday number (C mol^{-1})
i	current density (A m^{-2})
K_{App}	apparent kinetic constant (s^{-1})
k_i	organic specific reaction rate (dm^3 mol^{-1} s^{-1})
K_d	specific reaction rate for oxidant decay (s^{-1})
k_m	mass transfer coefficient (m s^{-1})
k_{OH}	OH radicals deactivation specific reaction rate (s^{-1})
V_R	recirculating volume (m^3)
φ	parameter in Eq. (A.2) $\varphi = 1 + (ak_m^A/ak_m^C)$
β	ratio between bulk oxidation rate and total oxidation rate
COD	chemical oxygen demand (mgO_2 dm^{-3})
TOC	total organic carbon (mgC dm^{-3})
Re	Reynolds number $Re = (vd\rho/\mu)$
ε_{95}	Faradic yield $\varepsilon_{95} = (V/8)(\Delta COD/\Delta t)(F/iA)$
s	mean space time yield $s = (1/t_f)\int_0^{t_f}(1/12)(\partial TOC/\partial t)dt$ (mmol s^{-1} dm^{-3})
r	mean oxidation rate $r = (1/t_f)\int_0^{t_f}(1/32)(\partial COD/\partial t)dt$ (mmol s^{-1} dm^{-3})
ε_c	energy consumption (kW h m^{-3})
δ	diffusion layer thickness $\delta = (D_i/k_m)$ (m)

Superscripts

DL	diffusion layer
B	bulk
OX	active chlorine species
OH	OH radicals
A	anodic
C	cathodic
S	anode surface

system, through the values of the kinetic constants, were quantified.

Our research group also implemented a model to describe the oxidation of chloride at BDD anodes [16]. The results showed that at low chloride concentration electrolysis with BDD produces a mixture of oxidant: low current density, high mass transfer and low residence time were the conditions to maximize the concentration of oxidants [16].

In the present work the electrochemical oxidation of m-cresol assumed as a model of phenolic substance was studied. m-Cresol is classified by the US EPA as persistent, priority and toxic chemical [17]: biological degradation of cresols was achieved only at long retention times, usually in days [18]. Thermal decomposition of cresols at 460 °C resulted in the formation of toxic intermediates [19,20]. The Fenton process was successfully applied to the removal of cresols; short chain aliphatic acids were obtained as final products [17]. Removal of about 90% of cresols with 67% of

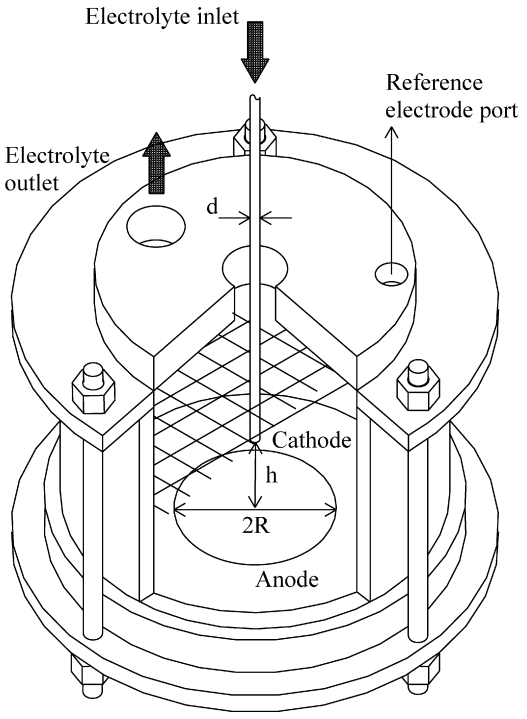

Fig. 1. Schematic view of the electrochemical cell.

energy efficiency was achieved by electrochemical treatment with BDD anodes [21], similar performances were achieved by a solar photoelectro-Fenton process with BDD anode [22].

The behaviour of m-cresol and its oxidation by-products is studied here. An important issue investigated is the effect of reactions involving chlorides and products of chlorides oxidation on organic oxidation. A mathematical model was formulated by combining the approaches used in the previous studies [15,16] accounting for the bulk and surface reactions occurring during electrolyses of waters containing chlorides.

2. Experimental

An impinging-jet-electrochemical cell (Fig. 1) was used, consisting of a section of Teflon pipe (10 cm high, and 10 cm inner diameter). p-type semiconducting BDD (film thickness 1.15 μm) supplied by ADAMANT, was used as anode (R = 5 cm).

The nozzle diameter (d) was 6 mm and the distance between the nozzle exit and the anode surface (h) was 0.5 cm. A grid of steel parallel to the anode and a saturated calomel electrode (SCE) constituted the cathode and the reference electrode, respectively.

The cell was inserted into a hydraulic circuit in which the electrolyte was pumped by a centrifugal pump from the reservoir to the cell and back in a closed loop. Flow rates ranged from 0.55 to 2.1 dm^3 min^{-1} which correspond to Reynolds numbers of 1950 and 7450, respectively. The values of Reynolds number were calculated by the following equation:

$$Re = \frac{vd\rho}{\mu} \quad (1)$$

where the diameter of the nozzle (d) was used as characteristic length. The runs were carried out at constant temperature (25 °C) controlled by a heat exchanger inserted in the hydraulic circuit.

The anodic and cathodic mass transfer coefficients were determined by the well-established limiting-current technique for the

ferro/ferricyanide redox couple; the value of k_m was obtained as

$$k_m = \frac{i_L}{zFC^b} \quad (2)$$

where z is the number of electrons involved in the process, F is the Faraday number (F = 96,500 C/eq) and C^b is the bulk concentration of the reactant.

The anodic mass transfer coefficient ($k_m{}^A$) was determined by measuring the limiting-current densities for 1 mM $K_4Fe(CN)_6$ oxidation in presence of an excess of $K_3Fe(CN)_6$ (0.1 M) in order to ensure that the cathodic reaction never became the limiting process. An excess of $K_4Fe(CN)_6$ was guaranteed during measurements of the cathodic mass transfer coefficient ($k_m{}^C$). The supporting electrolyte utilised for the limiting-current measurements was Na_2CO_3 0.5 M [23].

By assuming that the value of dynamic viscosity for the diluted aqueous solutions is not influenced by the electrolyte composition, and in particular by 200 mg dm^{-3} of chlorides, the values of mass transfer coefficients for the ith species (k_{mi}) only depend on the chemistry of the species and they were evaluated from the values of the ferro/ferricyanide redox couple (k_{m0}) [24].

$$k_{mi} = k_{m0}\left[\frac{D_i}{D_0}\right]^{2/3} \quad (3)$$

where D_i and D_0 are the relevant diffusion coefficients.

Galvanostatic electrolyses were performed with solutions containing 100 mg dm^{-3} of m-cresol and 100 mg dm^{-3} of NO_3^- as supporting electrolyte. Depending on the runs the solutions also contained 200 mg dm^{-3} of Cl^-. Electrolyses were also performed with solutions only containing chloride and nitrate ions. pH of the solutions was monitored during the runs, appreciable variations from neutrality were not observed.

Anodic current density values ranging from 5 to 10 mA cm^{-2} were imposed by means of a galvanostat (AMEL – 2049). The value of applied current density was selected to achieve an anodic potential higher than 2.7 V (vs. SCE), which is the minimum potential for H_2O oxidation [9].

During electrolyses, qualitative and quantitative analyses of m-cresol and its oxidation intermediates were carried out by HPLC (UV detector (270 nm); column Chrompack Chromsphere 5 C8; mobile phase, CH_3OH + 0.1% H_3PO_4 and 0.05 M KH_2PO_4 + 0.1% H_3PO_4 = 50:50; flow rate, 1.7 cm^3 min^{-1}; column temperature, 25 °C). Identification of chromatographic peaks was performed by comparison with pure standards. The trend of mineralization was monitored by measuring the total organic content (TOC) by a Shimatzu TOC 500A instrument.

The oxidant concentration expressed as mg dm^{-3} of active chlorine was measured by the DPD method [6]. Ion concentrations of Cl^- and its ionic oxidation products were measured by ion chromatography (Metrohm 761, conductivity detector) with a 6.1006.430 Metrosep Anion supp. 4 column (mobile phase 2 mM $NaHCO_3$/1.3 mM Na_2CO_3, flow rate 1.5 cm^3 min^{-1}). The identification of the different species was accomplished on the basis of the retention times and the quantification was performed by external calibration.

3. Results and discussion

Fig. 2 shows the trend with time of the fraction of m-cresol removed during galvanostatic electrolyses at 5 mA cm^{-2}, different electrolyte flow rates, and with and without chloride ions. The inset shows the semi-logarithmic plot of the normalised concentration of m-cresol vs. time.

Removal of the reactant higher than 90% was achieved in all the examined conditions. At values of Re of 7450, the removal of m-cresol was fast and almost complete after 20 ks of treatment.

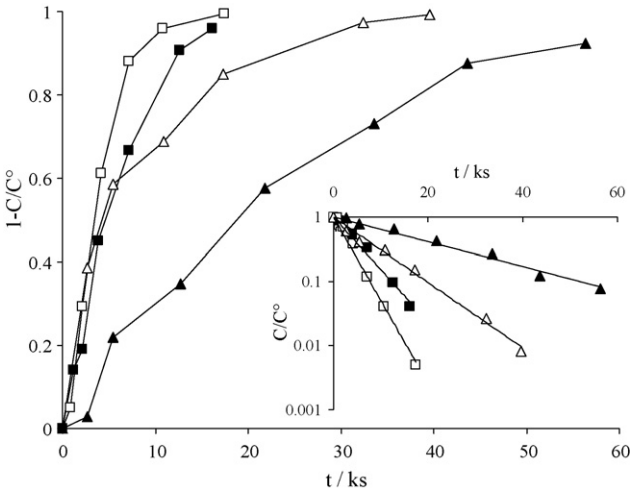

Fig. 2. Trend with time of the removed m-cresol concentration during galvanostatic electrolyses at 5 mA cm^{-2}, without chloride ions (full symbols) and with 200 mg dm^{-3} of chloride ions (empty symbols) and different recirculating flow rates: Re = 1950 (Δ, ▲); Re = 7450 (□, ■). Inset shows the trend with time of the normalised concentration of m-cresol.

Moreover an increase of the removal was observed in presence of chlorides, the other experimental conditions being the same.

Fig. 3 shows the trend of TOC, normalised with respect to the initial value, as a function of the m-cresol removal: removal of reactant being the same, higher values of mineralization ratio were obtained at the low flow rates.

The figure shows that all the values of TOC/TOC^0 are in the upper part of the graph, indicating that the process occurred through the formation of reaction intermediates. Aromatic and aliphatic intermediates were observed during electrochemical oxidation of phenol and phenolic compounds [25–27], polyhydroxybenzenes [28], 4-nitrophenol [29] and bisphenol A [30]. The distribution of these intermediates depended on the operative conditions, in particular on the ratio γ between the current density and the limiting-current density for the mineralization of the reactant [9]. Under the experimental conditions adopted in this work, the value of γ was always lower than one, which suggested that the removal of m-cresol occurred through intermediate formation: these results

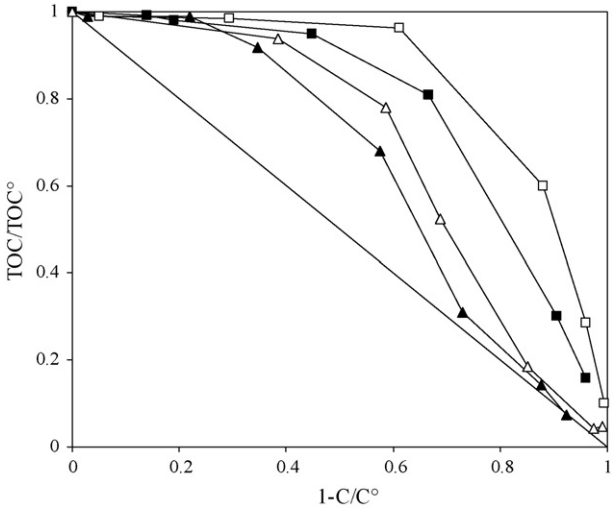

Fig. 3. Trend of the total organic carbon, normalised with respect to the initial value, as a function of the fraction of m-cresol removed during electrolyses at 5 mA cm^{-2}, without chloride ions (full symbols) and with 200 mg dm^{-3} of chloride ions (empty symbols) at different recirculating flow rates: Re = 1950 (Δ, ▲); Re = 7450 (□, ■).

Table 1
Values of the specific reaction rates and mass transfer coefficients in the relevant experimental conditions.

Re	C_{Cl^-} /mg dm^{-3}	$K_{App} \times 10^5$/m s^{-1}	R^2	$ak_m \times 10^5$/m s^{-1}
1950	0	4.55	0.98	5.01
1950	200	11.71	0.99	5.01
7450	0	18.86	0.99	19.11
7450	200	29.82	0.98	19.11

are in agreement with those obtained by Flox et al. [22–31] during the electrochemical oxidation of m-cresol at BDD anodes.

In the present work HPLC analyses showed the presence of phenolic compounds that disappeared during the runs. At the end of the process a mixture of carboxylic acids, mainly consisting in maleic and oxalic acid, was obtained.

As it can be observed from the inset of Fig. 2, in the examined operative conditions, the trend of m-cresol concentration followed a pseudo-first-order kinetics:

$$\ln\frac{C_m}{C_m^0} = -\frac{A}{V}K_{App}t \quad (4)$$

where C_m^0 is the initial concentration of reactant, and K_{App} is the specific reaction rate.

Table 1 shows the values of the specific reaction rates K_{App} obtained by linear regression of experimental data. When the electrolyses were performed without chloride ions, satisfactory agreement between K_{App} and the values of mass transfer coefficient at the relevant Re numbers was obtained; this indicated that the disappearance of the reactant was controlled by the mass transfer towards the anodic surface, as it was observed in other works [32].

When the galvanostatic electrolyses were performed in presence of 200 mg dm^{-3} of chloride ions the values of the pseudo-first-order constant were higher than those obtained without chlorides, the operative conditions being the same. This indicated the presence of a further mechanism, different from the pseudo-surface oxidation. At BDD anodes electrochemical oxidation of chlorides allowed the formation of active chlorine species (HClO, ClO_2) [16], which gave a bulk contribution depending on the reactivity of the organics towards active chlorine. The reactivity of the substituted phenols, as m-cresol, is connected with the Hammett's constant which reflects the electron density on the aromatic ring ($HClO/ClO^-$) [33]; the value of Hammett's constant of m-cresol is negative indicating that a partial oxidation by means of active chlorine is possible [34].

Removal of reactant being the same, the mineralization measured in presence of chlorides was low (see Fig. 3), indicating that reaction intermediates were less reactive than m-cresol towards active chlorine.

Fig. 4 shows the values of active chlorine concentration obtained at different electrolysis time by DPD method. The concentration of oxidants decreased as the anodic current density increased: this can be explained by considering that the main mechanism of active chlorine conversion to chlorate and chlorites [6,10,35] is the oxidation by OH radicals in the anodic reaction zone, which rate increases with current density [16]. In this work higher values of oxidant concentrations were obtained in the electrolyses performed at the highest values of Re. High values of Re resulted in a fast removal of active chlorine from the anodic zone, so limiting its oxidation to chlorate by OH radicals [16].

A mathematical model was then implemented to simulate the behaviour of the system, based on the following assumptions.

- The kinetic path of organic degradation was represented by three sequential steps: the first led to cyclic intermediates (CI), the second was the oxidation of these by-products to aliphatic acid (AI), the third was the mineralization.

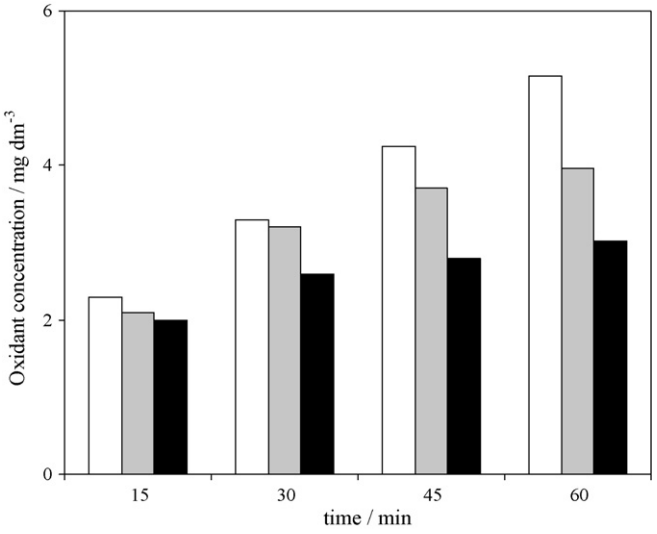

Fig. 4. Oxidant concentration obtained at different electrolysis time from solution containing 200 mg dm^{-3} of chloride ions: Re = 7450, i = 5 mA cm^{-2} (white bars); Re = 1950, i = 5 mA cm^{-2} (grey bars); Re = 1950, i = 10 mA cm^{-2} (black bars).

$$\text{m-cresol} \Rightarrow \text{CI} \Rightarrow \text{AI} \Rightarrow CO_2$$

- All the oxidative steps occurred through chemical reactions in liquid phase, mediated by OH radicals or by active chlorine species. The reaction rates for each step were expressed by a second-order kinetics with respect to the concentrations of the ith organic compound (C_i) and the oxidising compound (C_O) as follows:

$$R = k_i C_i C_O \quad (5)$$

- The behaviour of chlorine compounds was represented by the electrochemical oxidation of chloride ions to chlorine, followed by the formation of the active chlorine species (OX) in liquid phase. The formation of more oxidised species (PCl), such as chlorates was the final step of chlorine oxidation:

$$Cl^- \Rightarrow Cl_2 \Rightarrow \text{OX} \Rightarrow \text{PCl}$$

The mass balances for both organic compounds and chlorine compounds were written for the diffusion layer and the bulk of the solution: the equations are reported in the appendix together with the boundary conditions and the details of the model implementation.

Table 2 shows the values of the parameters utilised in the model, along with the corresponding sources: the values obtained in this work were the adjustable parameters of the model. Values were calculated through sensitivity analysis from the trend with time of the concentrations of the different species. Each constant was obtained by a single set of experimental data; literature values were used as initial values [16,36].

The model predictions were then validated through comparison with experimental data obtained from galvanostatic electrolyses under different conditions: examples of comparison between model predictions and experimental data are reported in the following figures.

Results related to the behaviour of chloride, active chlorine species and more oxidised chlorine species are shown in Fig. 5a–d.

The proposed model allowed quantitative interpretation of the effects of the operative parameters on the process with a

Table 2
Parameters for the numerical solution of the mathematical model proposed.

				Source
Kinetic constants $dm^3\ mol^{-1}\ s^{-1}$	Reaction with OH radicals	m-cresol	1.4×10^{10}	Ross et al. [36]
		Aromatic intermediates	9×10^{8}	This work
		Aliphatic acids	0.7×10^{8}	Ross et al. [36]
		Active chlorine species	5×10^{9}	This work
	Reaction with active chlorine species	m-cresol	1.2×10^{4}	This work
		Aromatic intermediates	5.5×10^{3}	This work
		Aliphatic acids	9×10^{2}	This work
OH radicals deactivation kinetic constant/s^{-1}			0.9×10^{10}	Mascia et al. [15]
Active chlorine deactivation kinetic constant/s^{-1}			9.7×10^{-4}	Polcaro et al. [16]
Diffusivity coefficients/$m^2\ s^{-1}$		Organic compounds	9.0×10^{-10}	Wilke and Chang correlation [37]
		OH radicals	2.3×10^{-10}	Kikuchi et al. [38]
		Chlorinated species	1.1×10^{-9}	Wilke and Chang correlation [37]
Faradic yield for chloride oxidation (η_{Cl})			0.2	This work
Parameter in Eq. (6) (φ)			1.2/1.5	This work

good agreement with experimental data. The increase of the concentration of oxidants with the recirculating flow rate, as well as the effect of current density were correctly predicted by the model.

Fig. 6a–d shows the results related to electrolyses of m-cresol solutions under different experimental conditions.

Fig. 6a and b compares the results obtained with different recirculating flow rates: the effect of the increased mass transfer rate on reactant removal and intermediates distribution was well accounted by the model. Data obtained from electrolyses in presence of chlorides (Fig. 6c and d) show the increase of reaction rate due to the bulk mechanism. Moreover, the effect of the different reactivity towards active chlorine species of cyclic and aliphatic intermediates and of m-cresol can be observed by comparing data obtained either in presence or in absence of chlorides. The prediction of the model was acceptable in all the examined conditions.

The model predictions allowed to estimate the contribute of the bulk reactions (β) to the overall removal rate for both the m-cresol and the total aromatic compounds. This estimation was done by calculating the ratio between the rate of oxidation in the bulk and the overall rate of oxidation:

$$\beta = 100 \times \frac{1}{t_f} \int_0^{t_f} \frac{(\partial C/\partial t)\big|_b}{(\partial C/\partial t)\big|_o} dt \tag{6}$$

Table 3 shows the values of β calculated under different operative conditions for the removal of m-cresol and for the total content of aromatic compounds.

As expected, the bulk contribute was a growing function of chloride concentration. Moreover it decreased as the surface reaction rate increased at the highest *Re* values. Since the current dedicated to chloride oxidation mainly depended on its concentration, for

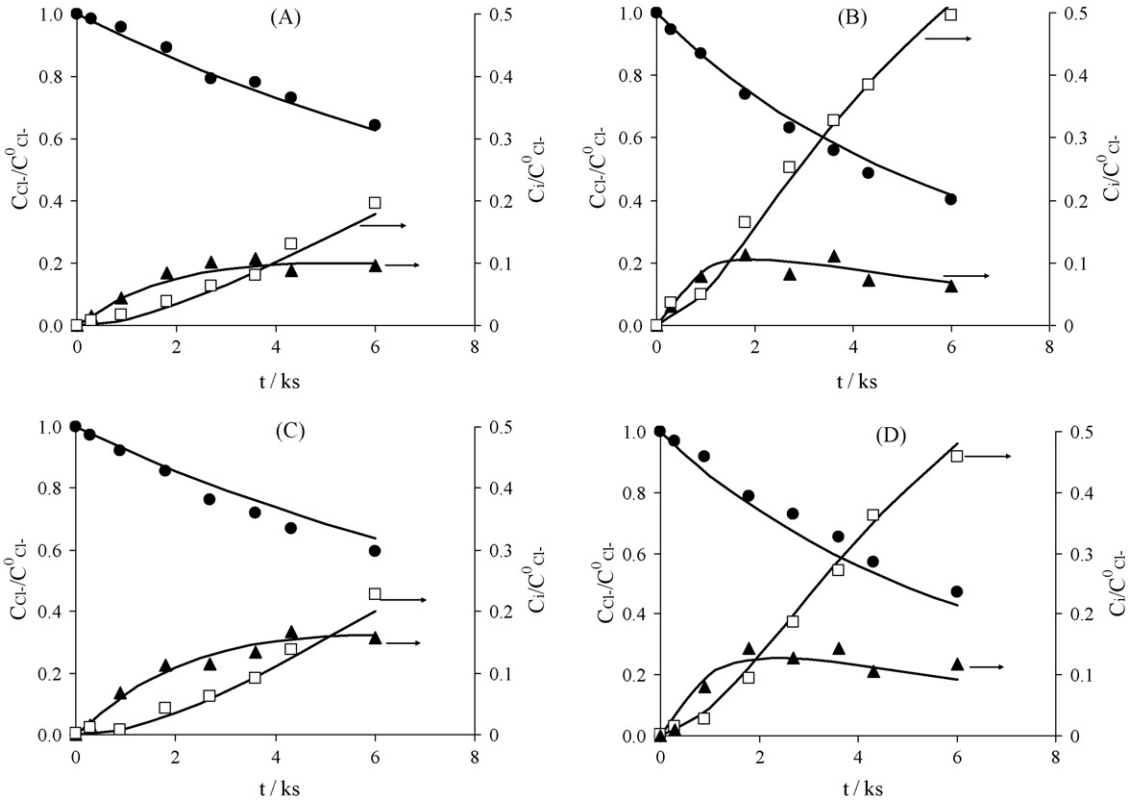

Fig. 5. Comparison between calculated (lines) and experimental data of chloride ions (●), oxidants (▲) and chlorate ions (□) concentrations during electrolyses under different operative conditions: (a) $i = 5\ mA\ cm^{-2}$, $Re = 1950$; (b) $i = 10\ mA\ cm^{-2}$, $Re = 1950$; (c) $i = 5\ mA\ cm^{-2}$, $Re = 7450$; (d) $i = 10\ mA\ cm^{-2}$, $Re = 7450$.

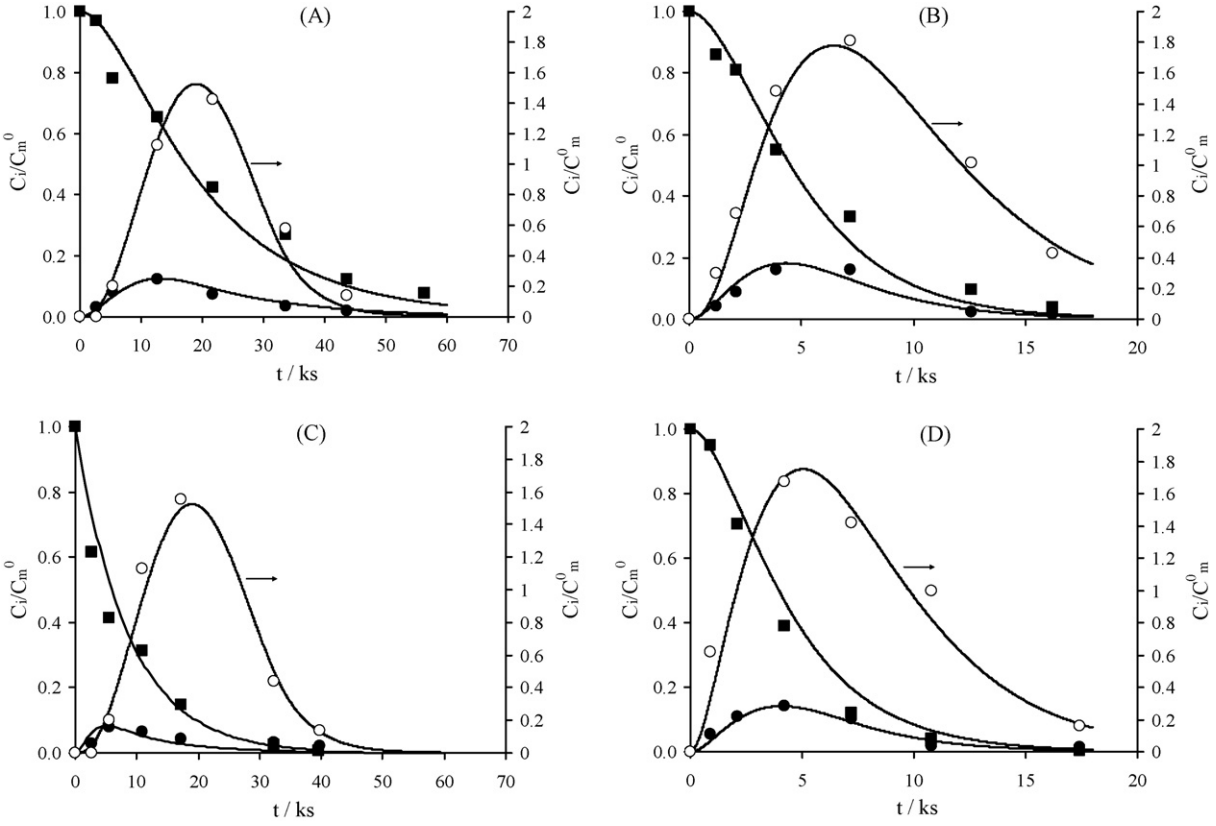

Fig. 6. Comparison between calculated (lines) and experimental data of m-cresol (■), cyclic intermediates (●) and aliphatic acids (○) concentrations as a function of time during electrolyses at 5 mA cm^{-2}: in solution without chloride ions (a and b) and with 200 mg dm^{-3} of chloride ions (c and d) at *Re* = 1950 (a and c) and *Re* = 7450 (b and d).

each value of Cl^- low values of β were observed at high current density when an excess of current for OH radicals generation was still guaranteed.

The model predictions were then utilised to individuate the optimum process conditions for the treatment of water containing a phenolic compound and chloride at different concentrations, by using some relevant figures of merit.

If the aim of the process is the simple removal of a compound, the faradic yield evaluated for 95% of removal (ε_{95}) may be considered

$$\varepsilon_{95} = \frac{V}{8}\frac{\Delta COD}{\Delta t}\frac{F}{iA} \tag{7}$$

However, if the process specifications require a high rate of organic removal during the whole process, the mean space time yield *s* should be also considered: in the constant volume system adopted in the present case, *s* may be expressed as

$$s = \frac{1}{t_f}\int_0^{t_f}\frac{1}{12}\frac{\partial \mathrm{TOC}}{\partial t}dt \tag{8}$$

where t_f is the electrolysis time at which 95% of TOC is removed from the solution.

Concerning the wastewater treatment, the aim of the process is often to reduce the organic load as chemical oxygen demand; in this case the total organic removal may be expressed as the mean oxidation rate of COD (*r*), which is a useful parameter when only partial mineralization is acceptable.

$$r = \frac{1}{t_{f1}}\int_0^{t_{f1}}\frac{1}{32}\frac{\partial \mathrm{COD}}{\partial t}dt \tag{9}$$

t_{f1} may be defined as the electrolysis time at which 90% of COD is removed from the solution.

Energy consumption was evaluated for 95% of TOC removal, by considering a cell potential of 4 V, as obtained from the experiments:

$$\varepsilon_C = \frac{\Delta E}{V} I t_f \tag{10}$$

Table 4 shows the values of the different figures of merit considered, calculated by the model at different *Re*, current density and chloride concentration.

The increase in *Re* still resulted in an increase of ε_{95} at low chloride concentration; when the content of chloride was high and the bulk oxidation was the main mechanism in the removal of the compound, low *Re* value were sufficient to achieve the process

Table 3
Values of β calculated under different operative conditions for the removal of the reactant and the aromatic compounds.

	$[Cl^-]$ mg dm^{-3}	i = 5 mA cm^{-2}			i = 10 mA cm^{-2}		
		Re			*Re*		
		2000	5000	7500	2000	5000	7500
$\beta_{\text{m-cresol}}$	200	50.5	46.6	40.8	33.0	32.4	25.0
	850	65.0	64.0	63.1	40.0	46.0	34.4
	2000	91.0	85.0	81.0	63.0	59.0	53.0
$\beta_{\text{aromatics}}$	200	20.0	19.4	8.1	20.0	13.1	5.0
	850	47.0	33.6	18.5	30.0	27.0	7.2
	2000	47.9	45.0	43.0	40.0	32.1	25.9

Table 4
Values of figures of merit calculated under different operative conditions.

	$[Cl^-]$ mg dm^{-3}	i = 5 mA cm^{-2}			i = 10 mA cm^{-2}		
		Re			*Re*		
		2000	5000	7500	2000	5000	7500
ε_{95}	0	0.31	0.71	0.94	0.21	0.42	0.53
	200	0.67	0.81	0.88	0.63	0.68	0.71
	850	0.41	0.64	0.63	0.52	0.57	0.59
	2000	0.23	0.40	0.40	0.20	0.38	0.40
s 10^5 mmol s^{-1} dm^{-3}	0	16.5	36.1	39.2	21.6	39.2	40.1
	200	13.0	29.8	30.8	34.5	47.3	65.3
	850	9.7	10.2	10.7	43.0	45.4	55.4
	2000	4.5	6.5	8.5	47.8	48.6	50.4
r 10^5 mmol s^{-1} dm^{-3}	0	19.7	44.4	54.7	26.2	54.7	54.3
	200	16.5	43.0	47.5	46.2	62.6	63.9
	850	14.2	18.1	15.7	64.9	67.0	68.7
	2000	6.3	8.7	11.8	68.0	70.8	71.5
ε_C kW h m^{-3}	0	8.89	3.78	2.71	13.32	7.12	7.55
	200	3.62	2.82	1.67	4.44	4.17	4.09
	850	4.44	1.84	1.87	4.02	4.10	4.50
	2000	5.82	4.44	4.44	3.99	3.87	3.15

specifications. Moreover from the values in the table an optimal value of Cl^- can be predicted at the different *Re* values.

It is worth to observe the low values of *s* which were obtained at low current density and high chloride content: under these conditions, the current was mainly dedicated to oxidation of Cl^- to active chlorine species and the surface concentration of OH radicals was low. This led to accumulation of such compounds as aliphatic acids, which are refractory towards oxidation by active chlorine. Similar behaviour was observed for the values of *r*, although in a less extent. High values of *r* and *s* were obtained at high current density: under these conditions an excess of current for OH radicals generation was still guaranteed.

The effect of chlorides and *Re* was also observed for the energy consumption: although high *Re* values led to low energy consumption, this effect was less evident at high chloride concentrations. The trend of energy consumption followed that of the space time yield: the energy consumption increased with the applied current density, and a positive effect of chlorides was observed at high values of current density.

4. Conclusions

The behaviour of the electrochemical process with BDD anodes was numerically predicted by the mathematical model developed in this work. The model predictions were compared with experimental data: a good agreement was obtained in all the examined conditions.

The model was then utilised to calculate some figures of merit usually adopted to characterise the process performances.

Results indicated that, depending on the process specifications, the optimal conditions are different:

- Low current density and high values of *Re* should be adopted if the aim of the process is the removal of a compound, without particular regard to the formation of intermediates.
- High *Re* values should be adopted if a partial oxidation of the organic fraction is requested such as for electrochemical process used as a pre-treatment, coupled with a biological treatment.
- High current density should be imposed in presence of high content of chloride ions to obtain acceptable reductions of COD or TOC.

An optimal value of chloride concentration can be found to minimise the energy consumption.

Acknowledgements

The authors acknowledge the financial support of Fondazione Banco di Sardegna.

Appendix A.

The electrochemical reactor was represented by a combination of a diffusion-reaction model, which simulated the anodic diffusion layer, and a stirred-tank reactor representing the bulk.

The volume of anodic diffusion layer (V_f) depended on the thickness of the Nernst diffusion layer δ ($V_f = A^*\delta$):

$$\delta = \frac{D}{k_m} \tag{A.1}$$

The volume of the bulk solution zone was equal to the overall recirculating volume.

Two anode reactions were considered: oxidation of water to OH radicals and of chlorides to active chlorine species (OX). The rates of the chemical reactions involving organics in liquid phase were described by second-order kinetics.

Mole balances of the *i*th organic compounds, active chlorine species and final products of chloride oxidation were written to model the bulk reactions. The cathodic reduction of OX was assumed as mass transfer controlled.

$$\begin{aligned}
\frac{dC_i^B}{dt} &= ak_m(C_i^S - C_i^B) + k_{i-1}^{OX}C_{i-1}^B C_{OX}^B - k_i^{OX}C_i^B C_{OX}^B \\
\frac{dC_{OX}^B}{dt} &= ak_m^A(C_{OX}^S - \varphi C_{OX}^B) - \sum_i k_i^{OX}C_i^B C_{OX}^B \\
\frac{dC_{PCl}^B}{dt} &= ak_m^A(C_{PCl}^S - C_{PCl}^B)
\end{aligned} \tag{A.2}$$

where φ depends on the ratio between anodic and cathodic specific mass transfer rates

$$\varphi = 1 + \frac{ak_m^A}{ak_m^C} \tag{A.3}$$

The chloride concentration was assumed as uniform in the whole reactor and only time-dependent:

$$-V_r \frac{dC_{Cl^-}}{dt} = \eta \frac{I}{2F} - A_c k_m^C C_{OX}^B - V_r K_d' C_{OX}^B \quad (A.4)$$

The mole balance of the ith compound in the diffusion layer was written as

$$\frac{\partial C_i^{DL}}{\partial t} = -D_i \frac{\partial^2 C_i^{DL}}{\partial x^2} + k_{i-1}^{OX} C_{i-1}^{DL} C_{OX}^{DL} - k_i^{OX} C_i^{DL} C_{OX}^{DL} + k_{i-1}^{OH} C_{i-1}^{DL} C_{OH} - k_i^{OH} C_i^{DL} C_{OH} \quad (A.5)$$

where the terms on the right side represent diffusion, generation and consumption of the ith compound.

The inactivation of chlorinated oxidants was represented by a second-order kinetics in which the constant $k^{OH\text{-}OX}$ was a lumped parameter used to account for the decay of OX.

$$\frac{\partial C_{OX}^{DL}}{\partial t} = -D_{OX} \frac{\partial C_{OX}^{DL}}{\partial x^2} - \sum_i k_i^{OX} C_i^{DL} C_{OX}^{DL} - k^{OH\text{-}OX} C_{OH} C_{OX}^{DL}$$
$$\frac{\partial C_{PCl}^{DL}}{\partial t} = -D_{PCl} \frac{\partial C_{PCl}^{DL}}{\partial x^2} + k^{OH\text{-}OX} C_{OH} C_{OX}^{DL} \quad (A.6)$$

A first-order kinetics was adopted to describe the reactions of OH radicals to give oxygen and a lumped kinetic constant k^{OH} was used [15].

$$\frac{dC_{OH}^{DL}}{dt} = -D_{OH} \frac{\partial^2 C_{OH}^{DL}}{\partial x^2} - \sum_i k_i^{OH} C_i^{DL} C_{OH} - k^{OH\text{-}OX} C_{OX}^{DL} C_{OH} - k_{OH} C_{OH} \quad (A.7)$$

Eqs. (A.2)–(A.7) were numerically solved with the following initial conditions:

$$C_{OH} = C_{OX}^{DL} = C_{OX}^B = 0$$
$$C_i^{DL} = C_i^B = C_{i0} \forall x \quad (A.8)$$

the boundary conditions for OH radicals and active chlorine at the anode surface were represented by the Faraday's law:

$$D_{OH} \frac{\partial C_{OH}}{\partial x} = -(1 - \eta_{Cl^-}) \frac{I}{AF} \quad (A.9)$$

The other boundary conditions were the following:

$$D_i \frac{\partial C_i^{DL}}{\partial x} = 0 \quad x = 0$$
$$C_i^{DL} = C_i^B \quad x = \delta$$
$$C_{OH} = 0 \quad x \Rightarrow \infty \quad (A.10)$$

The model equations were numerically solved by finite element software: the numerical solution of the equations allowed to predict the trend in time of the concentration of the different compounds in the bulk of solution, as well as the evolution of the space profile concentration of the considered species.

References

[1] M.F. Wu, G.H. Zhao, M.F. Li, L. Liu, D. Li, Applicability of boron-doped diamond electrode to the degradation of chloride-mediated and chloride-free wastewaters, J. Hazard. Mater. 163 (2009) 26–31.

[2] P. Canizares, B. Louhichi, A. Gadri, B. Nasr, R. Paz, M.A. Rodrigo, C. Saez, Electrochemical treatment of the pollutants generated in an ink-manufacturing process, J. Hazard. Mater. 146 (2007) 552–557.

[3] E. Brillas, I. Sires, C. Arias, P.L. Cabot, F. Centellas, R.M. Rodriguez, J.A. Garrido, Mineralization of paracetamol in aqueous medium by anodic oxidation with a boron-doped diamond electrode, Chemosphere 58 (2005) 399–406.

[4] P. Rychen, L. Pupunat, W. Haenni, E. Santoli, Water treatment applications with BDD electrodes and the DiaCell (R) concept, New Diamond Front. Carbon. Technol. 13 (2003) 109–117.

[5] A.M. Polcaro, A. Vacca, M. Mascia, P. Palmas, R. Pompei, S. Laconi, Characterization of a stirred tank electrochemical cell for water disinfection processes, Electrochim. Acta 52 (2007) 2595–2602.

[6] M.E.H. Bergmann, J. Rollin, Product and by-product formation in laboratory studies on disinfection electrolysis of water using boron-doped diamond anodes, Catal. Today 124 (2007) 198–203.

[7] P. Cañizares, J. Garcia-Gomez, J. Lobato, M.A. Rodrigo, Modeling of wastewater electro-oxidation processes part II. Application to active electrodes, Ind. Eng. Chem. Res. 43 (2004) 1915–1931.

[8] J. Iniesta, P.A. Michaud, M. Panizza, G. Cerisola, A. Aldaz, C. Comninellis, Electrochemical oxidation of phenol at boron-doped diamond electrode, Electrochim. Acta 46 (2001) 3573–3578.

[9] A.M. Polcaro, A. Vacca, S. Palmas, M. Mascia, Electrochemical treatment of wastewater containing phenolic compounds: oxidation at boron-doped diamond electrodes, J. Appl. Electrochem. 33 (2003) 885–892.

[10] A.M. Polcaro, A. Vacca, M. Mascia, F. Ferrara, Product and by-product formation in electrolysis of dilute chloride solutions, J. Appl. Electrochem. 38 (2008) 979–984.

[11] J. Hastie, D. Bejan, M. Teutli-Leon, N.J. Bunce, Electrochemical methods for degradation of Orange II (sodium 4-(2-hydroxy-1-naphthylazo) benzenesulfonate), Ind. Eng. Chem. Res. 45 (2006) 4898–4904.

[12] A. Cabeza, A.M. Urtiaga, I. Ortiz, Electrochemical treatment of landfill leachates using a boron-doped diamond anode, Ind. Eng. Chem. Res. 46 (2007) 1439–1446.

[13] M. Panizza, P. Michaud, G. Cerisola, C. Comninellis, Electrochemical treatment of wastewaters containing organic pollutants on boron-doped diamond electrodes: prediction of specific energy consumption and required electrode area, Electrochem. Commun. 3 (2001) 336–339.

[14] J. Iniesta, P. Michaud, M. Panizza, G. Cerisola, A. Aldaz, C. Comninellis, Electrochemical oxidation of phenol at boron-doped diamond electrode, Electrochim. Acta 46 (2001) 3573–3578.

[15] M. Mascia, A. Vacca, S. Palmas, A.M. Polcaro, Kinetics of the electrochemical oxidation of organic compounds at BDD anodes: modelling of surface reactions, J. Appl. Electrochem. 37 (2007) 71–76.

[16] A.M. Polcaro, A. Vacca, M. Mascia, S. Palmas, J. Rodriguez Ruiz, Electrochemical treatment of waters with BDD anodes: kinetics of the reactions involving chlorides, J. Appl. Electrochem. doi:10.1007/s10800-009-9870-x.

[17] V. Kavitha, K. Palanivelu, Destruction of cresols by Fenton oxidation process, Water Res. 39 (2005) 3062–3072.

[18] P.Y.A. Ahamad, A.A.M. Kunhi, Degradation of high concentrations of cresols by *Pseudomonas* sp. CP_4, World J. Microbiol. Biotechnol. 11 (1999) 661–664.

[19] C.J. Martino, P.E. Savage, J. Kasiborski, Kinetics and products from o-cresol oxidation in supercritical water, Ind. Eng. Chem. Res. 34 (1995) 1941–1951.

[20] C.J. Martino, P.E. Savage, Thermal decomposition of substituted phenols in supercritical water, Ind. Eng. Chem. Res. 36 (1997) 1385–1390.

[21] J.L. Nava, F. Nunez, I. Gonzalez, Electrochemical incineration of p-cresol and o-cresol in the filter-press-type FM01-LC electrochemical cell using BDD electrodes in sulfate media at pH 0, Electrochim. Acta 52 (2007) 3229–3235.

[22] C. Flox, P.L. Cabot, F. Centellas, J.A. Garrido, R.M. Rodriguez, C. Arias, E. Brillas, Solar photoelectro-Fenton degradation of cresols using a flow reactor with a boron-doped diamond anode, Appl. Catal. B 75 (2007) 17–28.

[23] R. Greef, R. Peat, L.M. Peter, D. Pletcher, J. Robinson, Instrumental Methods in Electrochemistry, Ellis Horwood, Chichester, 1985.

[24] F. Walsh, A First Course in Electrochemical Engineering, The Electrochemical Consultancy, Romsey, 1993.

[25] B. Nasr, G. Abdellatif, P. Canizares, C. Saez, J. Lobato, M.A. Rodrigo, Electrochemical oxidation of hydroquinone, resorcinol, and catechol on boron-doped diamond anodes, Environ. Sci. Technol. 39 (2005) 7234–7239.

[26] A. Morao, A. Lopes, M.T.P. de Amorim, I.C. Goncalves, Degradation of mixtures of phenols using boron doped diamond electrodes for wastewater treatment, Electrochim. Acta 49 (2004) 1587–1595.

[27] P. Canizares, M. Diaz, J.A. Dominguez, J. Garcia-Gomez, M.A. Rodrigo, Electrochemical oxidation of aqueous phenol wastes on synthetic diamond thin-film electrodes, Ind. Eng. Chem. Res. 41 (2002) 4187–4194.

[28] P. Canizares, C. Saez, J. Lobato, M.A. Rodrigo, Electrochemical oxidation of polyhydroxybenzenes on boron-doped diamond anodes, Ind. Eng. Chem. Res. 43 (2004) 6629–6637.

[29] P. Canizares, C. Saez, J. Lobato, M.A. Rodrigo, Electrochemical treatment of 2,4-dinitrophenol aqueous wastes using boron-doped diamond anodes, Electrochim. Acta 49 (2004) 4641–4650.

[30] M. Murugananthan, S. Yoshihara, T. Rakuma, T. Shirakashi, Mineralization of bisphenol A (BPA) by anodic oxidation with boron-doped diamond (BDD) electrode, J. Hazard. Mater. 154 (2008) 213–220.

[31] C. Flox, C. Arias, E. Brillas, A. Savall, K. Groenen-Serrano, Electrochemical incineration of cresols: a comparative study between PbO_2 and boron-doped diamond anodes, Chemosphere 74 (2009) 1340–1347.

[32] M. Panizza, G. Cerisola, Removal of colour and COD from wastewater containing acid blue 22 by electrochemical oxidation, J. Hazard. Mater. 153 (2008) 83–88.

[33] Z. Xiuping, S. Shaoyuan, W. Junjun, L. Fanxiu, Z. Huazhang, K. Jiangtao, H. Qi, N. Jinren, Electrochemical oxidation characteristics of p-substituted phenols using a boron-doped diamond electrode, Environ. Sci. Technol. 41 (2007) 6541–6546.

[34] M. Deborde, U. von Gunten, Reactions of chlorine with inorganic and organic compounds during water treatment—kinetics and mechanisms: a critical review, Water Res. 42 (2008) 13–51.

[35] M.E.H. Bergmann, T. Iourtchouk, K. Schops, K. Bouzek, New UV irradiation and direct electrolysis—promising methods for water disinfection, Chem. Eng. J. 85 (2002) 111–117.

[36] F.D. Ross, A.B. Ross, Selected Specific Rates of Reactions of Transient From Water in Aqueous Solution. III. Hydroxyl Radical and Perhydroxyl Radical and their Radical Ions, U.S. Dept. of Commerce, Washington, 1977.
[37] R.H. Perry, D.W. Green, Perry's Chemical Engineers' Handbook, Mc Graw Hill, New York, 1997.
[38] Y. Kikuchi, K. Sunada, T. Iyoda, K. Hashimoto, A. Fujishima, Photocatalytic bactericidal effect of TiO_2 thin films: dynamic view of the active oxygen species responsible for the effect, J. Photochem. Photobiol. A 106 (1997) 51–56.